Stability of Lagrange Points: James Webb Space Telescope

Cacolici, Gianna Nicole; Hanson, Jake; Lejoly, Cassandra; Pearson, Kyle Alexander; Reynolds, Katherine

ABSTRACT

We continue to present a detailed procedure for analyzing the stability of Lagrange points both analytically and computationally. We verified the stability both analytically in a 2D Earth-Sun system, and computationally with a 3D N-body code. We tested the stability over several periods of time and plotted the path the orbits would take in such case. We also discuss the consequences of these stabilities with respect to the James Webb Space Telescope.

I. INTRODUCTION

Astronomy has been as a subject studied by humans for a few thousands of years. One of the most fascinating parts of astronomy is the study of the retrograde motion of the planets in the sky. Among the earliest recorded studies of the motion of planets was by Ptolemy around the year 150 CE (Jones). Ptolemy's geocentric model of the universe was accepted for many centuries following his death. This model placed the Earth at the center of the universe with the Sun and planets rotating around the Earth in epicycles. It was not until Copernicus came along (1473-1543) that the idea of a heliocentric system came along. He believed that the size of the planets' orbits was proportional to the distance from the Sun (Rabin 2004). This model, which features the Sun in the center and the planets rotating around it, was not accepted initially, but became the accepted belief of the universe.

It was not long until the telescope was invented and people started to truly record the motion of the planets. Tycho Brahe was one of the first to build an observatory to study the planets. He made very detailed observations of the planets and was able to predict their motions with an accuracy never seen before (Van Helden 1995). His results were published after his death and were used by Johannes Kepler, his student, to create the laws of planetary motion, which make use of elliptical orbits. To this day, this is the accepted idea of how planets orbit our Sun. These motions, although predicted by Kepler's Laws, can be predicted by Newton's Laws of Gravity. These explain how orbits can be stable.

These orbits are not the only places where objects can exist. Joseph-Louis Lagrange was the first to publish his theories of how three bodies can interact in a system (Lagrange 1772). Although the three body problem is not solvable analytically, Lagrange was able to determine points where all the forces balance out. An object placed at these "Lagrange points" feels no force. These are the points we will be studying in our paper.

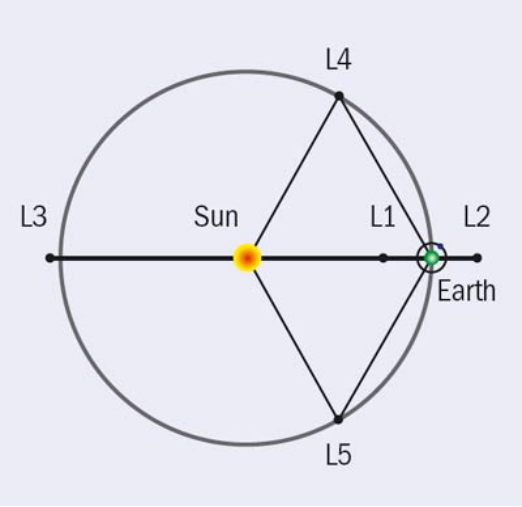

(*http://www.labspaces.net/blog/895/The_Lagrange_points_____Nature___s_parking_spots)*

There are five points in which all the forces balance out between two large bodies. For the purpose of this project, the Lagrange points considered will be those caused by the Sun and Earth. The Lagrange points all occur on the same 2D plane. The first three are in a straight line that passes through the Sun and Earth. The first point, labeled L1, occurs between the two bodies, L2 occurs just beyond the Earth, with both points occurring an equal distance from the Earth. L3 is found outside Earth's orbital path beyond the Sun. The last two points are located in the Earth's path via equilateral triangles. L4 is in line with where the Earth is rotating to and L5 is found trailing behind. All of these points are in constant rotation along with the Earth. The points are able to be viewed as they are in the diagram above by adopting a co-rotating frame. This frame holds the Sun and Earth fixed allowing for an easier visualization of the problem. The positions of the five Lagrange points are as follows:

(assuming that $\alpha = \frac{M_2}{M_1+M_2}$)

Point	**Location**
L1	$\left(R\left[1-\left(\frac{\alpha}{3}\right)^{\frac{1}{3}}\right],0\right)$
L2	$\left(R\left[1+\left(\frac{\alpha}{3}\right)^{\frac{1}{3}}\right],0\right)$
L3	$\left(-R\left[1-\left(\frac{5\alpha}{12}\right)^{\frac{1}{3}}\right],0\right)$
L4	$\left(\frac{R}{2}\left[\frac{M_1-M_2}{M_1+M_2}\right],\frac{\sqrt{3}}{2}R\right)$
L5	$\left(\frac{R}{2}\left[\frac{M_1-M_2}{M_1+M_2}\right],-\frac{\sqrt{3}}{2}R\right)$

Our study of Lagrange points can be applied to the James Webb Space Telescope (JWST) since it will be placed at the Earth-Sun L2 point. JWST is set to launch in 2018 and will be the successor to the Hubble Space Telescope and Spitzer Space Telescope. Since 1990, Hubble has been capturing light from the UV, visible, and near-IR, covering wavelengths from 0.1 to 1.7 microns. JWST will aim to improve previous work by acquiring more precise measurements in the IR spanning 0.6 to 29 microns.

As light from stars and galaxies travels through space, its wavelength increases. Therefore, by capturing light with longer-wavelengths, JWST will be able to see objects that are farther away from Earth and from farther back in the history of the universe. Since it will be able to capture images from farther back in time, the goal of the JWST will be to investigate the formation of stars and galaxies, as well as what happened after the formation of the universe. Specifically, it has four main science themes. The theme "First Light" will be investigating the formation of the first bright objects in the universe. "Assembly of Galaxies" will explore how galaxies and dark matter formed. The other two science themes are "The Birth of Stars and Protoplanetary Systems," and "Planetary Systems and the Origins of Life." If the next "Earth 2.0" hasn't been found before JWST is launched, it will surely find it. Having a greater sensitivity at IR wavelengths than Hubble and Spitzer will allow the JWST to measure the transmission and emission spectra of planets more precisely. Measuring the amount of light at specific wavelengths that gets absorbed by a planet's atmosphere as it passes in front of a star in its line of sight can give insight on the chemical composition of the atmosphere. By specifically targeting IR wavelengths the JWST will be able to detect the presence of H20, CH4, CO and CO2 in the atmospheres of planets outside the solar system.

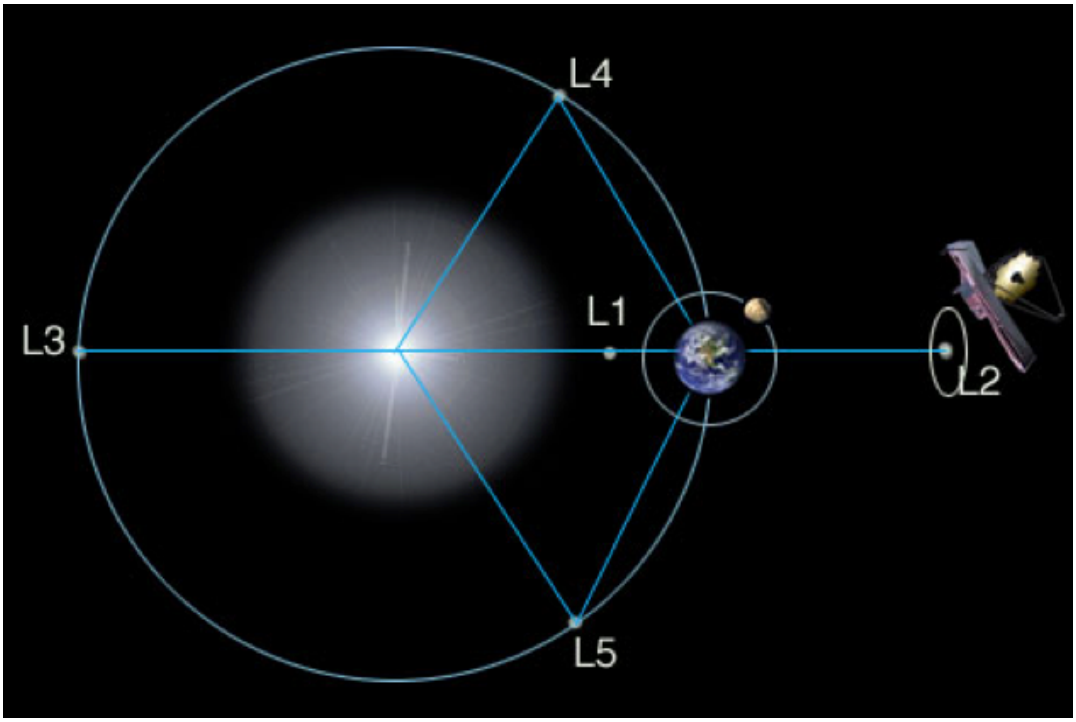

The James Webb Space Telescope will orbit the L2 Lagrange point. (*jwst.nasa.gov*)

Currently, the Hubble Space Telescope orbits the Earth at a distance of about 570 kilometers. JWST, however, will orbit the L2 Lagrange point, about 1.5 million kilometers away, as shown in the figure above. As the Earth orbits the Sun, JWST will orbit with it, maintaining a constant position relative to the Sun and Earth. In addition to stability, this position has several advantages for an IR telescope. Its constant relative position means the Earth and Moon will never obscure the telescope's view. It is important for an IR telescope to stay cool (below 50 K on the instrument side of the telescope, as shown in the figure below), so the JWST makes use of a solar shield, essentially a large sheet of reflective material. Since the light from the Sun will come only from one direction, the solar shield can effectively block it.

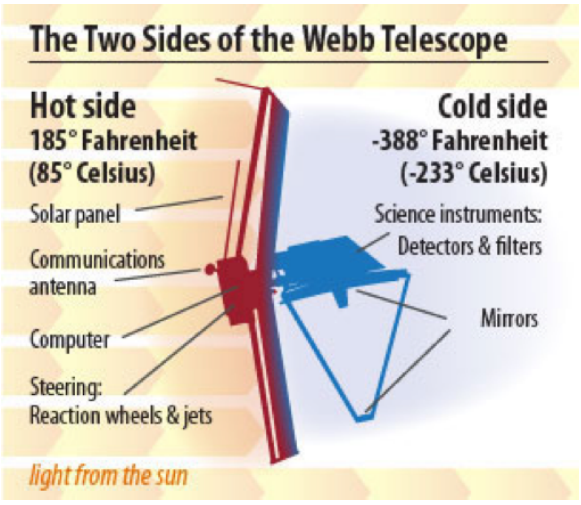

At the L2 Lagrange point, the solar shield can block the light and heat from the Sun. (*jwst.nasa.gov*)

In the second section, the stability of the Lagrange points will be analyzed analytically. The third section will show the results of the numerical model for the stability, and the timescales on which these are valid. The fourth section will outline the consequences of these results for the James Webb Space Telescope.

II. Analytic Stability of Lagrange Points

Having previously solved for the location of the five Lagrange points in the Earth-Sun system, our next task is to evaluate the stability of each. Since force is the negative gradient of a scalar potential, usually one can solve for stability by analyzing the shape of the effective potential at the point of interest. In our case, however, this method of analysis does not work because the coriolis force leads to a velocity dependent potential. Therefore, in order to analyze the stability we must linearize the equations of motion about each Lagrange point, and solve for small perturbations from equilibrium. In other words, we begin with:

$$x = x_i + \delta x\,, \quad v_x = \delta v_x\,,$$
$$x = y_i + \delta y\,, \quad v_y = \delta v_y\,,$$

Since we are evaluating the stability about each Lagrange point, (x_i,y_i) refers to the coordinates of the Lagrange point whose stability we wish to calculate. For small perturbations, the linearized equation of motion is as follows:

$$\frac{d}{dt}\begin{pmatrix}\delta x\\ \delta y\\ \delta v_x\\ \delta v_y\end{pmatrix} = \begin{pmatrix} 0 & 0 & 1 & 0\\ 0 & 0 & 0 & 1\\ \frac{d^2U_\Omega}{dx^2} & \frac{d^2U_\Omega}{dx\,dy} & 0 & 2\Omega\\ \frac{d^2U_\Omega}{dy\,dx} & \frac{d^2U_\Omega}{dy^2} & -2\Omega & 0\end{pmatrix}\begin{pmatrix}\delta x\\ \delta y\\ \delta v_x\\ \delta v_y\end{pmatrix}.$$

It is important to note the the lower right block is due to the velocity dependent coriolis force, which did not make an appearance in solving for the Lagrange points because at that time we were solving for locations where the velocity was zero. With this in mind, we realize that the x and y component of the original inertial force are no more than the x and y derivative of the effective potential. Thus, we only need to take the x and y derivative of these components to solve the lower left block. With an analytic expression for the linearized evolution matrix, the next step is to evaluate the matrix at each Lagrange point, then use the eigenvalues of the equation to describe the stability.

Using the previously derived equation for the inertial force,

$$\vec{F_\Omega} = \Omega^2(x - \frac{(x+\alpha R)R^3}{((x+\alpha R)^2+y^2)^{\frac{3}{2}}} - \frac{\alpha(x-R)R^3}{((x-R)^2+y^2)^{\frac{3}{2}}})\hat{i}$$
$$+ \Omega^2(y - \frac{yR^3}{((x+\alpha R)^2+y^2)^{\frac{3}{2}}} - \frac{\alpha yR^3}{((x-R)^2+y^2)^{\frac{3}{2}}})\hat{j}$$

we take the partial derivatives with respect to x and y for the x and y components to obtain expressions for the lower left block of the linearized evolution matrix.

$$\frac{\partial^2 U_\Omega}{\partial x^2} = \frac{\partial}{\partial x}\left(\Omega^2(x - \frac{(x+\alpha R)R^3}{((x+\alpha R)^2+y^2)^{\frac{3}{2}}} - \frac{\alpha(x-R)R^3}{((x-R)^2+y^2)^{\frac{3}{2}}})\right)$$
$$= \Omega^2\left(-\frac{\beta R^3}{((\alpha R+x)^2+y^2)^{3/2}} + \frac{3\beta R^3(\alpha R+x)^2}{((\alpha R+x)^2+y^2)^{5/2}} - \frac{\alpha R^3}{((x-\beta R)^2+y^2)^{3/2}} + \frac{3\alpha R^3(x-\beta R)^2}{((x-\beta R)^2+y^2)^{5/2}} + 1\right)$$

$$\frac{\partial^2 U_\Omega}{\partial x \partial y} = \frac{\partial}{\partial y}\left(\Omega^2(x - \frac{(x+\alpha R)R^3}{((x+\alpha R)^2+y^2)^{\frac{3}{2}}} - \frac{\alpha(x-R)R^3}{((x-R)^2+y^2)^{\frac{3}{2}}})\right)$$
$$= \Omega^2\left(3R^3 y\left(\frac{\beta(\alpha R+x)}{((\alpha R+x)^2+y^2)^{5/2}} + \frac{\alpha(x-\beta R)}{((x-\beta R)^2+y^2)^{5/2}}\right)\right)$$

$$\frac{\partial^2 U_\Omega}{\partial y \partial x} = \frac{\partial}{\partial x}\left(\Omega^2(y - \frac{yR^3}{((x+\alpha R)^2+y^2)^{\frac{3}{2}}} - \frac{\alpha y R^3}{((x-R)^2+y^2)^{\frac{3}{2}}})\right)$$
$$= \Omega^2\left(3R^3 y\left(\frac{\beta(\alpha R+x)}{((\alpha R+x)^2+y^2)^{5/2}} + \frac{\alpha(x-\beta R)}{((x-\beta R)^2+y^2)^{5/2}}\right)\right)$$

$$\frac{\partial^2 U_\Omega}{\partial y^2} = \frac{\partial}{\partial y}\left(\Omega^2(y - \frac{yR^3}{((x+\alpha R)^2+y^2)^{\frac{3}{2}}} - \frac{\alpha y R^3}{((x-R)^2+y^2)^{\frac{3}{2}}})\right)$$
$$= \Omega^2\left(-\frac{\beta R^3}{((\alpha R+x)^2+y^2)^{3/2}} + \frac{3\beta R^3 y^2}{((\alpha R+x)^2+y^2)^{5/2}} - \frac{\alpha R^3}{((x-\beta R)^2+y^2)^{3/2}} + \frac{3\alpha R^3 y^2}{((x-\beta R)^2+y^2)^{5/2}} + 1\right)$$

Evaluating these expressions at the symmetrical points L1 and L2, we obtain the following results:

L1:	L2:
$\frac{\partial^2 U_\Omega}{\partial x^2} = -9\Omega^2$	$\frac{\partial^2 U_\Omega}{\partial x^2} = 9\Omega^2$
$\frac{\partial^2 U_\Omega}{\partial x \partial y} = 0$	$\frac{\partial^2 U_\Omega}{\partial x \partial y} = 0$
$\frac{\partial^2 U_\Omega}{\partial y \partial x} = 0$	$\frac{\partial^2 U_\Omega}{\partial y \partial x} = 0$
$\frac{\partial^2 U_\Omega}{\partial y^2} = 3\Omega^2$	$\frac{\partial^2 U_\Omega}{\partial y^2} = -3\Omega^2$

Therefore, the eigenvalues of the linearized evolution matrix are:

$$\lambda_{1,2} = \pm\sqrt{1+2\sqrt{7}}$$

Due to the symmetry of L1 and L2, it is to be expected that the eigenvalues for each are the same. Since one eigenvalue is real and positive and the other real and negative, we conclude that L1 and L2 are saddle points. They are not dynamically stable, meaning that small deviations from the exact equilibrium point will grow over time. Without corrections, an object perturbed slightly from L1 or L2 would drift away from the stable equilibrium.

Next, we analyze the stability at L3.

L3:

$$\frac{\partial^2 U_\Omega}{\partial x^2} = -3\Omega^2$$

$$\frac{\partial^2 U_\Omega}{\partial x \partial y} = 0$$

$$\frac{\partial^2 U_\Omega}{\partial y \partial x} = 0$$

$$\frac{\partial^2 U_\Omega}{\partial y^2} = \frac{7\alpha}{8\beta}\Omega^2$$

The eigenvalues from the linearized evolution matrix are:

$$\lambda_{1,2} = \pm\Omega\sqrt{\frac{3\alpha}{8\beta}}$$

Here α and β refer to the mass ratios of the Earth and Sun, respectively:

$$\alpha = \frac{M_E}{M_E+M_S} \qquad\qquad \beta = \frac{M_S}{M_E+M_S}$$

Since the Earth has a mass far smaller than that of the Sun, the eigenvalues are small numbers, approximately $\pm 2.625 \times 10^{-}6$. As for L1 and L2, evaluating the evolution matrix for L3 yields one real and positive eigenvalue and one real and negative eigenvalue, indicating a saddle point. It is similarly dynamically unstable. However, since the eigenvalue is much smaller in magnitude than those for L1 and L2, the instability is less dramatic. An object displaced slightly from L3 willd drift away from equilibrium much more slowly than it would if displaced the same amount from L1 or L2.

Analysis of L4 and L5 is slightly more complicated, as none of the partial derivatives cancel to zero. Since L4 and L5 are symmetric, the entries in the matrix are similar.

L4:

$$\frac{\partial^2 U_\Omega}{\partial x^2} = \frac{3}{4}\Omega^2$$

$$\frac{\partial^2 U_\Omega}{\partial x \partial y} = \frac{3\sqrt{3}}{4}(\beta-\alpha)\Omega^2$$

$$\frac{\partial^2 U_\Omega}{\partial y \partial x} = \frac{3\sqrt{3}}{4}(\beta-\alpha)\Omega^2$$

$$\frac{\partial^2 U_\Omega}{\partial y^2} = \frac{9}{4}\Omega^2$$

L5:

$$\frac{\partial^2 U_\Omega}{\partial x^2} = \frac{3}{4}\Omega^2$$

$$\frac{\partial^2 U_\Omega}{\partial x \partial y} = \frac{3\sqrt{3}}{4}(\alpha-\beta)\Omega^2$$

$$\frac{\partial^2 U_\Omega}{\partial y \partial x} = \frac{3\sqrt{3}}{4}(\alpha-\beta)\Omega^2$$

$$\frac{\partial^2 U_\Omega}{\partial y^2} = \frac{9}{4}\Omega^2$$

The eigenvalues, then, are:

$$\lambda_{1,2} = \pm i\frac{\Omega}{2}\sqrt{2 - \sqrt{27(\beta - \alpha)^2 - 23}}$$

Because the mass of the Sun is much greater than the mass of the Earth, β is much greater than α, and the eigenvalues are all imaginary, with no real components. This result indicates that L4 and L5 are stable.

It is interesting to note that evaluation of only the bottom left 2 x 2 portion of the matrix, involving the effective potential, yields two positive eigenvalues. This would indicate an unstable node. However, because the system is rotating and not stationary, the coriolis force affects objects near L4 and L5, pulling them toward the point if they are perturbed. Therefore, L4 and L5 are actually stable equilibrium points.

III. NUMERICAL SIMULATION TESTING STABILITY

In order to verify our analytical solution we created a 3D N-body code to assess the stability regions of our solution. Our code is written using a combination of Python and C/C++. All of the plotting and setting up of initial conditions was done in Python and we outsource the computational work to C++. To conserve energy and accuracy in our code we invoke a fourth order method for updating the position and velocity. The fourth order method is formally known as the fourth order Hermite which is an implicit method that uses a predictor-corrector scheme. Please reference our midterm report for the exact computational formulation we adopt.

We tested two different models of the Earth-Sun system to assess the stability of each of the Lagrange points. The first model we tested was one where the initial positions of the bodies placed at the Lagrange points were not perturbed. See Figure 1. Using this model we can compute the stability of each of the points by analyzing the drift timescale or e-folding time. Small departures from equilibrium will grow exponentially with an e-folding time of roughly 1/eigenvalue for the associated Lagrange point. By fitting a function of the form A*exp(B*t) to the distance of a body from its initial point as a function of time we can obtain the drift timescale as 1/B. Below is a table containing the drift times for the 3 unstable Lagrange points. The optimal function was found using the Levenberg-Marquardt minimization algorithm which uses a damped least squares method to solve nonlinear least squares problems.

Point	Drift Time (Computational)	Drift Time (Analytical)
L1	24.9 Days	~23 Days
L2	24.4 Days	~23 Days
L3	43.12 Years	~150 Years

From this result our computationally derived drift time more or less coincides with our analytically derived answer. You can see that a body placed at L1 or L2 will wander off after a few months unless some corrections are made. However if you have a body at L3 it will need far less adjustment compared to L1 or L2 to maintain a steady orbit. The reason being is that the L3 point is not influenced by the gravitational potential of the Earth as much as L1 or L2.

In the second model each body was randomly perturbed using a gaussian distribution centered on the position of the associated Lagrange point and given a variance equal to 0.01% of its position element. See Figure 2 for one of the trial perturbation runs. In this model we tested the boundary of each Lagrange point by perturbing the initial position of the body. Our results are rather hand-wavy since a full Monte Carlo simulation is needed to robustly determine the sensitivity of the boundaries around the Lagrange points. Assessing the energy contour plot is better suited for determining the orbital paths of various bodies. See Figure 3.

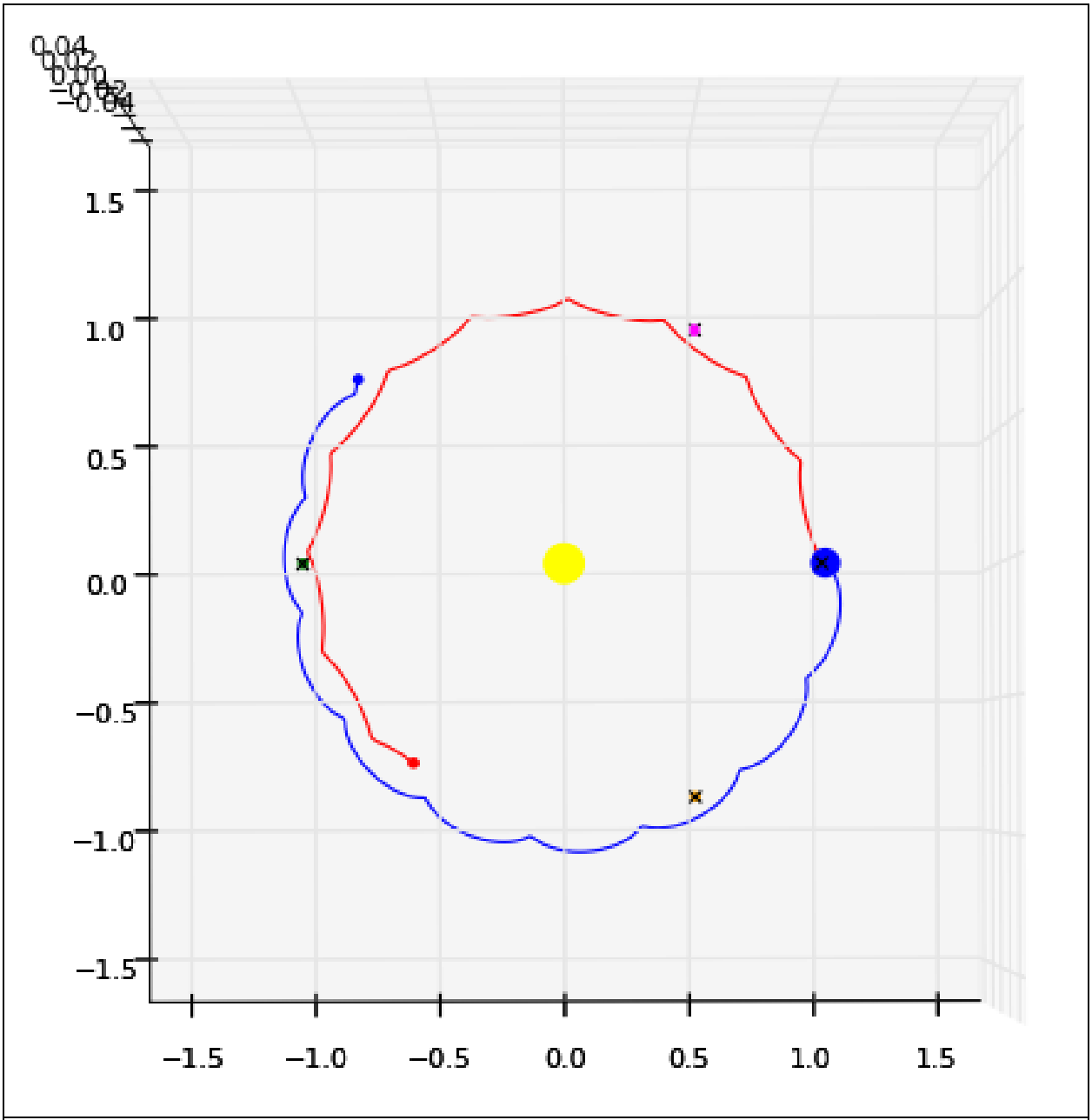

Figure 1. Orbits of Lagrange points in a co-rotating frame after 10 years where the initial positions were not perturbed from equilibrium.

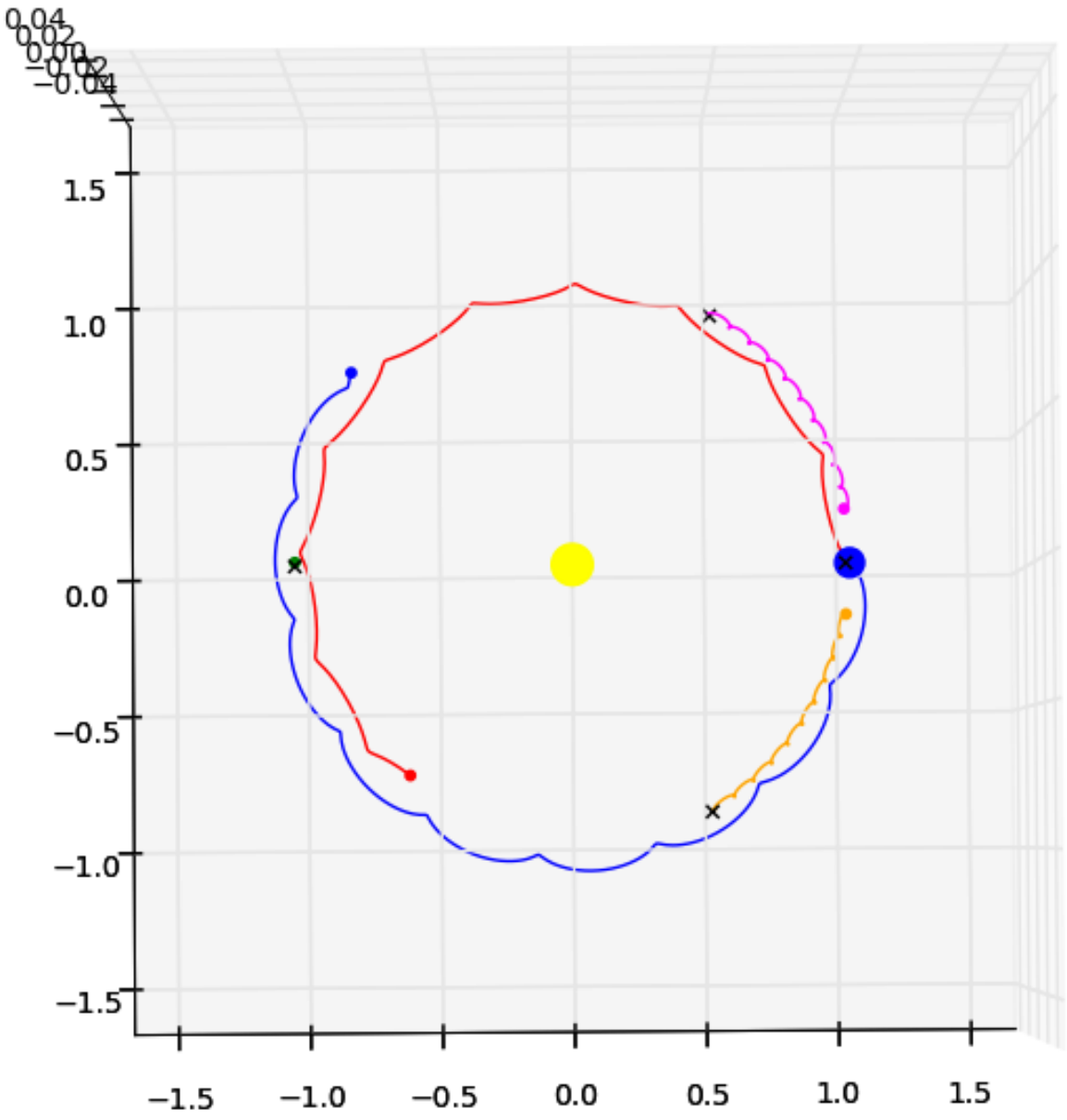

Figure 2. Orbits of Lagrange points in a co-rotating frame. This plot shows the orbital paths of mock James Webb Space Telescopes at the Lagrange points for the Earth-Sun system after 10 years.

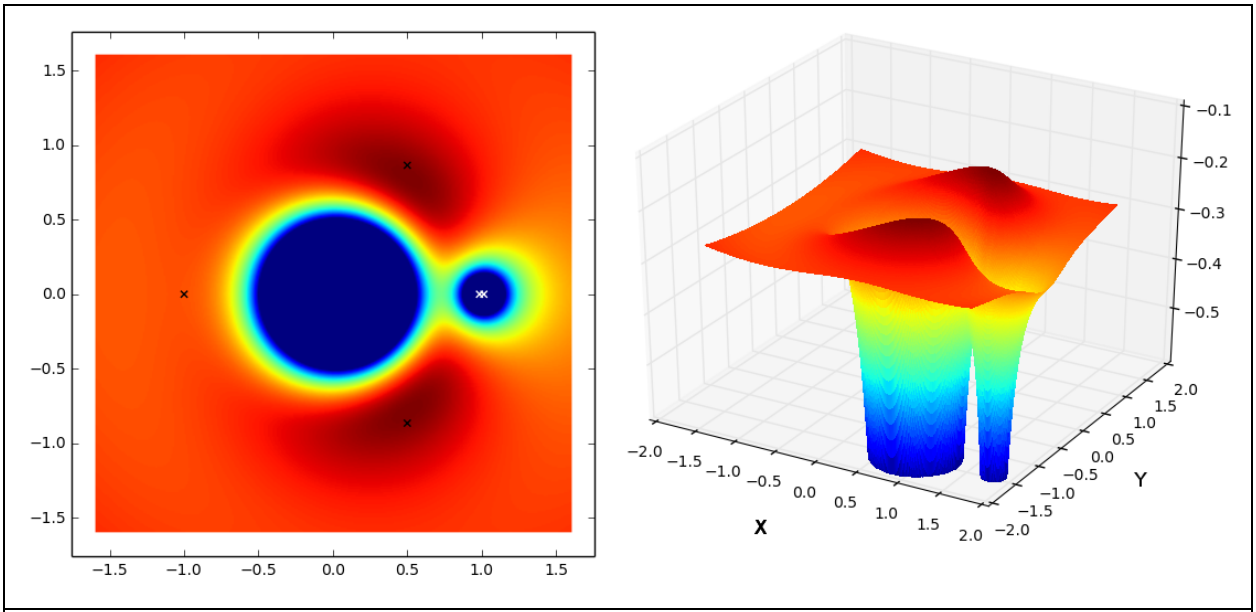

Figure 3. Energy Contour plot. Extrema of the generalized potential are marked with x's.

IV. CONSEQUENCES FOR THE JAMES WEBB SPACE TELESCOPE

The James Webb Space Telescope will be an instrumental part in mapping the infrared emission in our universe. Because of solar and Earth radiation, it needs to have a shield protecting its detectors. One of the best ways to do this efficiently while still mapping the whole sky would be to place this space telescope on a line from the Earth to the Sun but on either side of the two objects. To limit the amount of energy necessary to keep this telescope in orbit around the Sun, it is necessary to place at one of the Lagrange points of the Earth-Sun system. Either L2 or L3 would place it at an ideal location for observations.

We have shown above both analytic and computational analysis of the stability of these two Lagrange points. Computationally we see that L2 is stable on the order of a month while L3 is stable for more than four decades. In the project overview, it is said that the JWST will be located at the L2 point for at least five years, although the goal is to reach 10 (Sabelhaus).

Knowing this, we would assume that the best location for the JWST would be L3 because that is the most stable. However, this is not the case and we can wonder why. There are several factors that come into this. First of all, L2 is much easier to reach from Earth than L3, thus it would require much less fuel to start with. Secondly, if there is a problem with the telescope, it would be much easier to fix it at L2, since it is closer to Earth. Thirdly, if we place an object exactly opposite the Sun, there would be no way to transmit data from it to us since the Sun would be in the way. Incidentally, this is also why

there are many science fiction works that place a small planet or an alien base at L3 – we have no way of seeing it.

All this being said, L2 is the obvious of the two choices. The stability is a problem that is not too difficult to solve. With technology nowadays, it is possible to change the path of the JWST to place it back at its equilibrium every few weeks with engines of some kind.

V. CONCLUSION

Our project has shown many aspects of the stability of Lagrange points both analytically and computationally. It is shown that only L4 and L5 are stable in a rotating system, while L1, L2, and L3 are all unstable. L3 is more stable than L1 or L2 by many years though, and is a perfect candidate for aliens to hide from us. We have also learned what will become of the James Webb Space telescope once placed at L2 and that its course needs to be adjusted at least every few weeks.

VI. REFERENCES

Cornish, Niel J. "The Lagrange Points." University of Montana, n.d. Web. 01 Mar. 2014. <http://www.physics.montana.edu/faculty/cornish/lagrange>.

Jones, Alexander Raymond. "Ptolemy (Egyptian Scientist and Mathematician)." *Encyclopedia Britannica Online.* Encyclopedia Britannica, n.d. Web. 21 Mar. 2014.

Lagrange, Joseph-Louis. "Le Probleme Des Trois Corps." *Itas-vis*. N.p., 1772. Web. 21 Mar. 2014. <http://www.Itas-vis.ulg.ac.be/cmsms/uploads/File/Lagrange_essai_3corp.pdf>

"Newton's Law of Gravitation." *Newton's Law of Gravitation*. N.p. 1997. Web. 21 Mar. 2014. <http://theory.uwinnipeg.ca/physics/circ/node7.html>.

Rabin, Sheila. "Nicolaus Copernicus." *Stanford University*. Stanford University, 30 Nov. 2004. Web. 19 Mar. 2014

Sabelhaus, Phillip A. and Decker, John, E. "An overview of the James Webb Space Telescope (JWST) project", *Proc. SPIE*5487, Optical, Infrared, and Millimeter Space Telescopes, 550 (October 12, 2004); doi:10.1117/12.549895; http://dx.doi.org/10.1117/12.549895

Van Helden, Al. "The Galileo Project | Science | Tycho Brahe." *The Galileo Project*. N.p., 1995. Web. 18 Mar. 2014